ARMY RESEARCH LABORATORY

Modeling of Toroidal Ordering in Ferroelectric Nanodots

by Joshua C. Crone and Peter W. Chung

ARL-TR-4165 **June 2007**

NOTICES

Disclaimers

The findings in this report are not to be construed as an official Department of the Army position unless so designated by other authorized documents.

Citation of manufacturer's or trade names does not constitute an official endorsement or approval of the use thereof.

DESTRUCTION NOTICE—Destroy this report when it is no longer needed. Do not return it to the originator.

Army Research Laboratory
Aberdeen Proving Ground, MD 21005-5066

ARL-TR-4165 **June 2007**

Modeling of Toroidal Ordering in Ferroelectric Nanodots

Joshua C. Crone and Peter W. Chung
Computational and Information Sciences Directorate, ARL

REPORT DOCUMENTATION PAGE

Form Approved
OMB No. 0704-0188

1. REPORT DATE *(DD-MM-YYYY)*	2. REPORT TYPE	3. DATES COVERED (From - To)
June 2007	Final	July 2006 to May 2007

4. TITLE AND SUBTITLE

Modeling of Toroidal Ordering in Ferroelectric Nanodots

5a. CONTRACT NUMBER

5b. GRANT NUMBER

5c. PROGRAM ELEMENT NUMBER

6. AUTHOR(S)

Joshua C. Crone and Peter W. Chung (both of ARL)

5d. PROJECT NUMBER
7UH7CL

5e. TASK NUMBER

5f. WORK UNIT NUMBER

7. PERFORMING ORGANIZATION NAME(S) AND ADDRESS(ES)

U.S. Army Research Laboratory
Computational and Information Sciences Directorate
Aberdeen Proving Ground, MD 21005-5066

8. PERFORMING ORGANIZATION REPORT NUMBER

ARL-TR-4165

9. SPONSORING/MONITORING AGENCY NAME(S) AND ADDRESS(ES)

10. SPONSOR/MONITOR'S ACRONYM(S)

11. SPONSOR/MONITOR'S REPORT NUMBER(S)

12. DISTRIBUTION/AVAILABILITY STATEMENT

Approved for public release; distribution is unlimited.

13. SUPPLEMENTARY NOTES

14. ABSTRACT

This report details progress and the completed study of ferroelectric properties in nanodots for potential application to toroidal ordering concepts in nonvolatile memory materials. The work was performed under support through the Student Temporary Employment Program at the U.S. Army Research Laboratory. Beginning with an introduction of basic concepts, the report reviews the current state-of-the-art of ferroelectric nanodot technology through a literature review and identifies areas of need for continued study. As part of the review, Ewald's summation for Coulomb interactions in periodic crystals, a critical contribution to the atomistic energy that enables the long-range ordering in ferroelectric solids, was derived and is presented in the appendix.

15. SUBJECT TERMS

band gap; crystals; modeling; photonics

16. SECURITY CLASSIFICATION OF:			17. LIMITATION OF ABSTRACT	18. NUMBER OF PAGES	19a. NAME OF RESPONSIBLE PERSON
a. REPORT	b. ABSTRACT	c. THIS PAGE			Joshua C. Crone
Unclassified	Unclassified	Unclassified	SAR	23	19b. TELEPHONE NUMBER (*Include area code*) 410-278-6027

Standard Form 298 (Rev. 8/98)
Prescribed by ANSI Std. Z39.18

Contents

List of Figures

Acknowledgments

The authors gratefully acknowledge partial support from the U.S. Army Research Laboratory's Major Shared Resource Center at the Computational & Informational Sciences Directorate, High Performance Computing Division, Computational Sciences & Engineering Branch through the Student Temporary Employment Program. Partial support is also gratefully acknowledged through the Joint Science and Technology Office of the Defense Threat Reduction Agency.

INTENTIONALLY LEFT BLANK

1. Introduction

The unique properties of ferroelectric materials have led to numerous studies aimed at incorporating ferroelectrics into memory devices. One particular application is the creation of non-volatile ferroelectric random access memory (NVFRAM). A ferroelectric material can maintain an induced polarization without an externally applied voltage, thus removing the need for a back-up disk and making the memory non-volatile (*1*). The ever-increasing demand for smaller memory devices has led to increased research in the field of ferroelectric nanostructures. Ferroelectric nanodots offer a potential increase in the storage density of NVFRAM from 0.2 gigabit per square inch (Gbit/in.^{2}) to 60 terabits per square inch, which is also four orders of magnitude greater than the 1-Gbit/in.^{2} capacity of current magnetic recording devices (*2*). The improved capacities for memory have inspired much interest in the properties and behavior of ferroelectric nanostructures. One area of interest is the toroidal ordering of dipoles in ferroelectric nanodots. This is a relatively unexplored field that appears promising yet requires extensive research before commercialization can be seriously considered.

2. Background on Ferroelectrics

Ferroelectric materials are in a unique category of materials defined by the appearance of spontaneous polarization. Ferroelectric crystals are a class of dielectric materials, which means they are semiconductors that have insulating and conductive properties. They may sustain internal electric dipole moments without an externally applied electric field. By contrast, dielectrics generally require an electric field to sustain a polarization. Ferroelectric properties also make them attractive for numerous applications in multifunctional electronic devices. Such properties include high dielectric constants, the pyroelectric effect, the electro-optical effect, and the piezoelectric effect.

Ferroelectric crystals become polarized when the positively charged central atom shifts in the opposite direction of the negatively charged oxygen atoms. Figure 1 illustrates how a non-polarized ferroelectric crystal becomes polarized. This phase transition only occurs below a critical temperature referred to as the Curie temperature or Curie point. The value of the Curie temperature varies for each material. Above this temperature, all ferroelectric crystals are nonpolar, or in a paraelectric state. Ferroelectrics under the Curie temperature exhibit multi-stable ground states. Therefore, they can change polarization directions through the application of an external electric field.

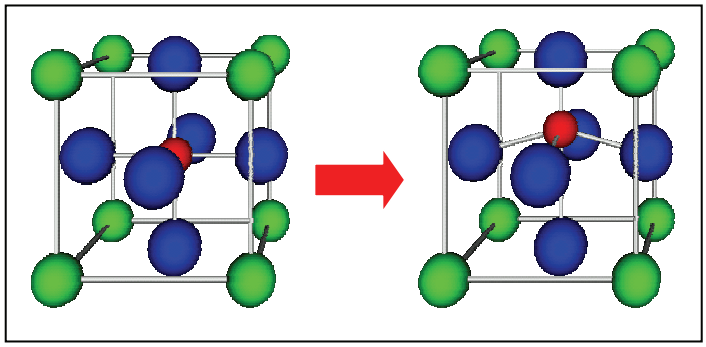

Figure 1. Schematic of the polarization phenomenon in a perovskite crystal cell (*3*).

Not all crystals in a structure share the same polarization directions. Regions of uniform dipole moments are referred to as domains, with the areas between them being domain walls. A wall separating two anti-parallel domains is a 180-degree wall, while a wall separating perpendicularly orientated dipoles is a 90-degree wall (both shown in figure 2). The total polarization of a ferro-electric structure is determined when the volume of the domains is summed in each direction. Ferroelectric domains are formed to minimize the electrostatic energy of depolarizing fields caused by surface charges (*4*). The switching of polarization is conducted through nucleation and domain-wall motion. The switching time is an important property for many applications and is limited by these two factors.

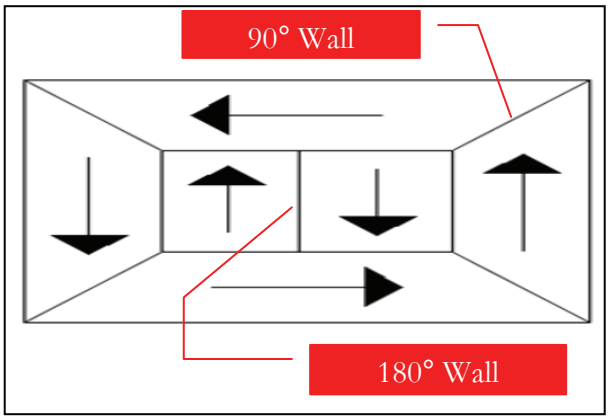

Figure 2. Polarization domains and domain walls in an inhomogeneously polarized material (*3*).

Figure 3 shows that the net polarization versus applied electric field produces a hysteresis loop. As an electric field is applied to a nonpolar ferroelectric, domains begin to switch until all domains point in the same direction (A). After the maximum polarization is reached, the electric field decreases and some of the domains switch back. At a zero electric field, more domains still have a positive polarization (B). The value at this point is the remnant polarization. As a negative field is applied, more domains become negative until the ferroelectric is completely nonpolar (C). The field required to reach a zero polarization is the coercive field. Finally, the field becomes more

negative until a maximum negative polarization is reached (D). The process is then reversed when we switch back to a positive electric field.

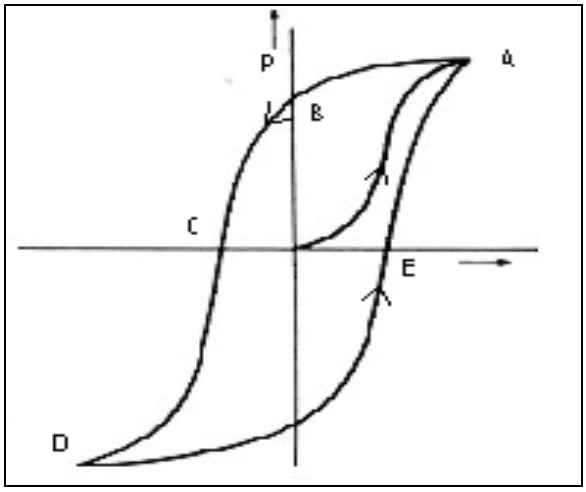

Figure 3. Hysteresis loop common to ferroelectric materials (*3*).

As a ferroelectric switches back and forth between the two polarized states, the maximum and remnant polarizations begin to decrease. This loss in switchable permanent polarization is ferroelectric "fatigue". Besides switching time and ferroelectric fatigue, a third factor affecting the use of ferroelectrics is dielectric breakdown. This occurs when an insulating material, such as a ferroelectric, is forced to conduct electricity in large electric fields. Dielectric strength measures the maximum electric field that a material can experience before dielectric breakdown occurs. The strength is measured in volts per unit length of thickness.

3. Background on Toroidal Ordering of Nanodots

The concept of toroidal ordering of ferroelectric nanodots began in 1946 with the work of Charles Kittel with ferromagnetic domains in small particles (*5*). His theory was based on the observation that the demagnetized state is the stable state in large ferromagnetic crystals in the absence of an applied magnetic field. To achieve a demagnetized state, a complex ordering of the domains is required. The ground state can be determined if the free energy equation is optimized in terms of the domain ordering. The free energy of the structure is given by the equation

$$F = F_W + F_M + F_a$$

The first term, F_W, represents the surface energy between domains and is calculated by

$$F_W = \sigma_W S$$

where σ_W is the surface energy per unit area and depends on the orientation of the boundary plane and the difference in spin direction across the boundary. The term, S, is the total area of the domain boundaries.

The second term in the free energy equation, F_M, is the magnetic field energy of the configuration or the work required to distribute the effective magnetic poles. The energy is calculated by

$$F_M = -\frac{1}{2}\int (\mathbf{H} \bullet \mathbf{M})\, dV$$

where **M** is the magnetic moment per unit volume (magnetization) and **H** is the resultant magnetic field. The integral is taken over the volume of the specimen.

The final term in the free energy equation, F_a, represents the anisotropy energy of spin orientation. This refers to the energy associated with a preferred axis of magnetization. It is calculated by

$$F_a = \rho_a V_a$$

where ρ_a is the anisotropy energy density of domains oriented in directions other than the direction of the easiest magnetization and V_a is the volume of those domains.

Two cases for small ferromagnetic nanodots were examined with the free energy equation. These cases were for a particle with one domain and for a particle with toroidally ordered domains. The first case had only magnetic energy since the domain was in the direction of preferred magnetization and there were no domain wall surfaces. Therefore, the energy could be described as

$$F \cong \frac{2\pi}{3} M_s{}^2 L^3$$

The energy for case two involved anisotropy energy and domain wall surface energy but had no net magnetization. Therefore, the energy could be described as

$$F = \sigma_W 2\sqrt{2}\, L^2 + \frac{\rho_a}{2} L^3$$

Through this process, it was discovered that the toroidal ordering results in the minimum energy for $L \geq 15\ nm$ using empirical estimations for the other variables.

4. Literature Review

The field remained relatively unexplored over the next 30 years until Zheludev et al. (*6*) first reported such structures. However, their work could never be reproduced and therefore, the study of toroidal ordering was again abandoned. A collection of papers between 1984 and 1985 extended

Kittle's work. These papers include Ginzburg et al. (*7*), Sannikov (*8*), and Sannikov and Zheludev (*9*). All these papers confirm the existence of toroidal moments in magnetism. A decade later, Gorbatsevich and Kopaev (*10*) and Sannikov (*11*) further extended the work. However, the work still remained relatively unnoticed until Naumov et al. (*2*) performed *ab initro* simulations on freely standing nano-particles of lead zirconate titanate. The simulations showed that phase transformations do occur in zero-dimensional particles (nanodots) and that the phase transformations lead to spontaneous toroidal moments under a critical temperature of approximately 600K. These toroidal moments occur to minimize the depolarizing field. Naumov et al. (*2*) found that two stable ground states exist for nanodots with a diameter larger than 3.2 nm and the states can be switched via a magnetic field rather than a static electric field as used for bulk ferroelectrics.

The work was continued by papers such as Ponomareva et al. (*11, 12*) and Prosandeev et al. (*13*). Ponomareva et al. published two papers in 2005 proposing models to examine the depolarizing fields (*4*) and effects of electrical and mechanical boundary conditions on ferroelectric nanoparticles (*12*). The atomistic models examine the depolarizing field and energy for ferroelectric nanostructures. They found the depolarizing field and energy by calculating the difference between dipole-dipole interactions for ferroelectric nanostructures during perfect open-circuit and short-circuit electrical boundary conditions. An open-circuit condition exhibits a maximum depolarizing field, while a short-circuit condition completely screens the effect of the depolarizing field. The energies calculated via their model were independent of dot size and agreed exactly with the established continuum approach. Through their simulations, Ponomareva et al. found that toroidal moments occur when the screening of the depolarizing field is less than 88% for a freely standing lead zirconate titanate nanostructure. After applying tensile and compressive strains of 2.65%, they discovered that toroidal moments occur under tensile strain with a screening of less than 88% but not under compressive strain. These results are illustrated in figure 4.

Prosandeev et al. (*13*) proposed a switching mechanism that uses inhomogeneous static electric fields to alter the toroidal moment of the nanodots without affecting the surrounding nanodots. They did this by placing two opposite dipolar sources at each end of the dot. This setup prevents any net polarization that could affect nearby nanodots. By rotating the source, they could switch the toroidal moment. The ability to switch the direction of the toroidal moment is vital for the integration of ferroelectric nanodots (FENs) into memory devices and other applications.

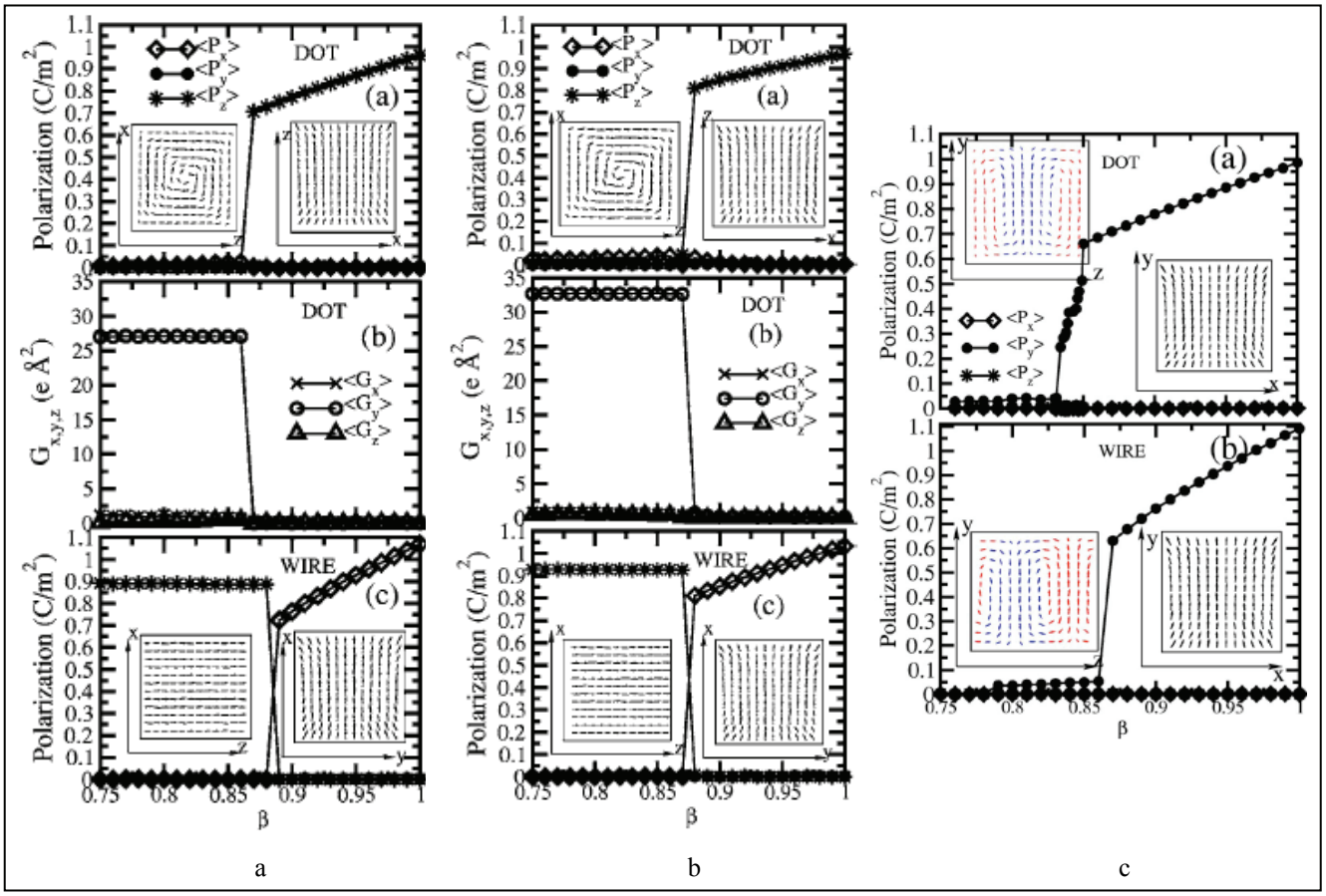

Figure 4. (a) Freely standing nanodot (b) FEN under tensile strain (c) FEN under compressive strain (*12*).

5. Advantages of Ferroelectric Nanodots

An obstacle for implementing FENs into NVFRAM is the understanding of the phase transformations on the nanoscale. In certain conditions, the polarization of nanodots is oriented toroidally rather than rectilinearly. The local dipoles are directed in a suitable direction to equilibrate the depolarizing field (*2*). The resultant orientation produces a toroidal moment. Various properties of the toroidally ordered nanodots are conducive for use in NVFRAM. The phase is bistable, meaning that two minimum energy states exist. These states can be easily translated to "0" or "1" in Boolean logic. Ground states can be switched with the use of a magnetic field that does not require contact with electrodes, which is challenging to create on the nanoscale (*2*). The local dipole orientation does not result in a net polarization; therefore, neighboring nanodots will not be affected when one nanodot switches polarization. All these properties make toroidally ordered FENs appealing to NVFRAM.

6. Future Work

The future of toroidally ordered ferroelectric nanodots in memory devices is bright. In principle, combining the properties shared by all ferroelectrics with those unique to toroidal ordering can lead to smaller, faster, and more reliable memory materials. However, more research must be performed on all aspects of their properties and behaviors before ferroelectric nanodots can be implemented. Among many mechanisms that remain unstudied, the interacting relationships among atomic structure, electromagnetic fields, and mechanical strains are not known. For example, the role of mechanical strains and thermal expansion on the stability of the toroids is unknown. Most importantly, it is still unclear if toroidal ordering has ever occurred experimentally since concepts have been posited mainly through theoretical models and calculations. Therefore, experimentation must accompany the theoretical calculations before ferroelectric nanodots are seriously considered for NVFRAM.

7. References

1. Auciello, O.; Scott, J.F.; Ramesh, R. The Physics of Ferroelectric Memories. *Physics Today* **July 1998**, *51* (7), 22-27.

2. Naumov, I.; Bellaiche, L.; Fu, H. Unusual Phase Transitions In Ferroelectric Nanodisks and Nanorods. *Nature* **2004**, *432*, 737.

3. Dragosits, Klaus. Structural Properties of Perovskites. Modeling and Simulation of Ferroelectric Devices, 2000. <http://www.iue.tuwien.ac.at/phd/dragosits/diss.html>.

4. Ponomareva, I.; Naumov, I.I.; Kornev, I.; Fu, H.; Bellaiche, L. Atomistic Treatment of Depolarizing Energy and Field in Ferroelectric Nanostructures. *Physical Review B* **2005**, *72*, 140102.

5. Kittel, Charles. Theory of the Structure of Ferromagnetic Domains in Films and Small Particles. *Physical Review* **1946**, *70*, 965.

6. Zheludev, I.S.; Perekalina, T.M.; Smirnovskaya, E.M.; Fonton, S.S.; Yarmukhamedov, Y.N. Magnetic Properties of Nickel-Boracite Iodide. *Journal of Experimental and Theoretical Physics Letters* **1974**, *20*, 129.

7. Ginzburg, V.L.; Gorbatsevich, A.A.; Kopayev, Y.V.; Volkov, B.A. On the Problem of Superdiamagnetism. *Solid State Communications* **1984**, *50* (4), 339-343.

8. Sannikov, D.G. Anomalies in the Dispersion of the Dielectric Susceptibility of Intrinsic Toroics. *Journal of Experimental and Theoretical Physics Letters* **1985**, *41*, 277.

9. Sannikov, D.G.; Zheludev, I.S. On the Possibility of Phase Transitions With Spontaneous Toroidal Moment Formation in Nickel Boracites. *Soviet Physics-Solid State* **1985**, *27*, 826.

10. Gorbatsevich, A.A.; Kopaev, Y.V. Toroidal Order in Crystals. *Ferroelectrics* **1994**, *161*, 321.

11. Sannikov, D.G. Ferrotoroic Phase Transitions in Boracites. *Ferroelectrics* **1998**, *219*, 177.

12. Ponomareva, I.; Naumov, I.I.; Bellaiche, L. Low-Dimensional Ferroelectrics Under Different Electrical and Mechanical Boundary Conditions: Atomistic Simulations. *Physical Review B* **2005**, *72*, 214118.

13. Prosandeev, S.; Ponomareva, I.; Kornev, I.; Naumov, I.I.; Bellaiche, L. Controlling Toroidal Moment by Means of an Inhomogeneous Static Field: An *Ab Initio* Study. *Physical Review Letters* **2006**, *96*, 237601.

8. Bibliography

1. Frenkel, Daan; Smit, Berend. *Understanding Molecular Simulations*, pp 292-300, Academic Press: San Diego, CA, 2002.
2. Gibbon, Paul; Sutmann, Sodehard. Long-Range Interactions in Many-Particle Simulations. *NIC Series* **2002**, *10*, 467-506.
3. Scott, J. F. Ferroeletrics: Novel Geometric Ordering of Ferroelectricity. *Nature* **2005**, *4*, 13.
4. Scott, J. F. Nanoferroelectrics: Statics and Dynamics. *Journal of Physics: Condensed Matter* **2006**, *18*, R361-R386.
5. Yoshioka, Daijiro. *Introduction to Statistical Physics*. Springer-Verlag: New York, 16 November 2006.

INTENTIONALLY LEFT BLANK

Appendix A. Derivation of Ewald Sum Equation

The following mathematical derivation was an assignment during the internship. The details of the method were uncovered to help us understand basic pedagogy of modeling ferroelectric systems from the atomistic level.

The Ewald sum is a means to calculate the electrostatic interactions of periodic systems. Its contribution to the total energy enables the formation of long range order and is the physical underpinning of ferroelectric polarization. The method involves superimposing a spherical Gaussian cloud on each ion in real space. These spherical clouds have a charge opposite the ion. A spherical Gaussian cloud is also superimposed on each ion in reciprocal space. These clouds have the same charge as the ion they surround. The Ewald sum calculation involves using Poisson's equation and Fourier transforms. The Ewald sum equation is comprised of a term to calculate short-range interactions in real space, a term to calculate long-range interactions in reciprocal space, and a correction term for self energy.

General Equation for Electrostatic Energy:

$$U = \frac{1}{2}\sum_{i}\sum_{j}\sum_{n}\frac{q_i q_j}{\left|r_i - (r_j + nL)\right|}$$

where 1/2 accounts for double counting of atom interactions
qi and qj are the charges on atoms i and j
ri and rj are the coordinates of atoms i and j in the unit cell
nL is the displacement vector for the different image cells

$$U = \frac{1}{2}\sum_{i} q_i \phi(r_i)$$

where $\phi(r_i)$ = Electric Potential at ri

$$\phi(r_i) = \sum_{j}\sum_{n}\frac{q_j}{\left|r_i - (r_j + nL)\right|}$$

Charge Density:

$\rho(r)$ = Point Charge – Gaussian Charge + Gaussian Charge

Density of Point Charge: $\rho(r) = \sum_{i} q_i \, \delta(r - r_i)$

where $\delta(r - r_i)$ is the Dirac delta function

Density of Gaussian Charge: $\rho(r) = \sum_i q_i \left(\frac{\alpha}{\pi}\right)^{3/2} e^{-\alpha(r-r_i)^2}$

where α is a parameter affecting the Gaussian width and affects computational efficiency

$$\rho(r) = \sum_i \left\{ \underbrace{q_i \left(\delta(r-r_i) - \left(\frac{\alpha}{\pi}\right)^{3/2} e^{-\alpha(r-r_i)^2} \right)}_{\text{Short Range Contributions}} + \underbrace{q_i \left(\frac{\alpha}{\pi}\right)^{3/2} e^{-\alpha(r-r_i)^2}}_{\text{Long Range Contributions}} \right\}$$

Electric Potential (Sh

$\phi_{short}(r) =$ Potential from Point Charge – Potential from Gaussian Charge

Potential from Point Charge: $\phi_{short,P}(r) = \sum_i \frac{q_i}{(r-r_i)}$

Potential from Gaussian Charge:

Poisson's Equation: $\nabla^2 \phi(r) = 4\pi\rho(r)$

$$\rho(r) = q_i \left(\frac{\alpha}{\pi}\right)^{3/2} e^{-\alpha(r-r_i)^2}$$

$$-\frac{1}{r}\frac{\partial^2 r\phi(r)}{\partial r^2} = 4\pi\rho(r)$$

$$-\frac{\partial\, r\phi(r)}{\partial r} = \int_\infty^r 4\pi r\, \rho(r)\, dr$$

$$= -\int_r^\infty 2\pi q_i \left(\frac{\alpha}{\pi}\right)^{3/2} e^{-\alpha r^2} dr^2$$

$$= -2\pi q_i \left(\frac{\alpha}{\pi}\right)^{3/2} \int_r^\infty e^{-\alpha r^2} dr^2$$

$$= -2q_i \left(\frac{\alpha}{\pi}\right)^{1/2} e^{-\alpha r^2}$$

$$r\phi(r) = 2q_i \left(\frac{\alpha}{\pi}\right)^{1/2} \int_0^r e^{-\alpha r^2} dr$$

$$\phi(r) = \frac{q_i}{r} erf(\sqrt{\alpha}\, r)$$

where erf is the error function and r=(r-ri)

$$\phi_{short}(r) = \sum_i \sum_n \frac{q_i}{|r-(r_i+nL)|} - \frac{q_i}{|r-(r_i+nL)|} erf\left(\sqrt{\alpha}\,(r-(r_i+nL))\right)$$

$$\phi_{short}(r) = \sum_i \sum_n \frac{q_i}{|r - (r_i + nL)|} erfc\left(\sqrt{\alpha}\left(r - (r_i + nL)\right)\right)$$

where erfc is the complimentary error function

Electrostatic Energy (Short Range):

$$U_{short} = \frac{1}{2}\sum_i \sum_j \sum_n \frac{q_i q_j}{|r_i - (r_j + nL)|} erfc\left(\sqrt{\alpha}\left(r_i - (r_j + nL)\right)\right)$$

Correction Term for Self Interaction:

$$\phi(r) = \frac{q_i}{r} erf\left(\sqrt{\alpha}\, r\right)$$

$$\phi(r = 0) = q_i \left(\frac{2}{\sqrt{\pi}}\right) e^{-\alpha r^2} \sqrt{\alpha}$$

By taking the limit as r approaches zero (using L'Hopital),

$$\phi_{self}(r_i) = 2q_i \left(\frac{\alpha}{\pi}\right)^{1/2}$$

$$U_{self} = \frac{1}{2}\sum_i q_i \phi_{self}(r_i)$$

$$U_{self} = \left(\frac{\alpha}{\pi}\right)^{\frac{1}{2}} \sum_i {q_i}^2$$

Electric Potential (Reciprocal Space):

Poisson's Eq: $-\nabla^2 \phi(r) = 4\pi\rho(r)$

Poisson's Eq after Fourier Transform: $k^2 \phi(k) = 4\pi\rho(k)$

$$\phi(k) = \frac{4\pi}{k^2}\rho(k)$$

$$\phi(r) = \sum_k \phi(k) e^{ikr}$$

$$\rho(k) = \frac{1}{V}\int_V \rho(r) e^{-ikr} dr$$

$$= \frac{1}{V}\int_V \sum_j \sum_n q_j \left(\frac{\alpha}{\pi}\right)^{\frac{3}{2}} e^{-\alpha r^2} e^{-ikr} dr$$

$$= \frac{q_j}{V}\left(\frac{\alpha}{\pi}\right)^{\frac{3}{2}} \int_{all\ space} e^{-\alpha\left(r^2 + \frac{ikr}{\alpha}\right)} dr$$

Side note: $\left(r^2+\frac{ikr}{\alpha}\right)=\left(r+\frac{ik}{2\alpha}\right)^2+\Psi$

$$\Psi=\left(\frac{k^2}{4\alpha^2}\right)$$

$$= \frac{q_j}{V}\left(\frac{\alpha}{\pi}\right)^{\frac{3}{2}}\int_{-\infty}^{\infty}e^{-\alpha\left[\left(r+\frac{ik}{2\alpha}\right)^2+\frac{k^2}{4\alpha^2}\right]}dr$$

Since the bounds of the integral are $-\infty,\infty$, $\left(r+\frac{ik}{2\alpha}\right)^2$ can be replaced by r^2

$$= \frac{q_j}{V}\left(\frac{\alpha}{\pi}\right)^{\frac{3}{2}}e^{\frac{-k^2}{4\alpha}}\int_{-\infty}^{\infty}e^{-\alpha r^2}$$

$$= \frac{q_j}{V}\left(\frac{\alpha}{\pi}\right)^{\frac{3}{2}}e^{\frac{-k^2}{4\alpha}}\left[\frac{\sqrt{\pi}}{2\sqrt{\alpha}}\left(erf(\infty)-erf(-\infty)\right)\right]$$

$$= \frac{q_j}{V}\left(\frac{\alpha}{\pi}\right)e^{\frac{-k^2}{4\alpha}}$$

In ref 12 $\frac{\alpha}{\pi}$ is omitted because of choice of units. This term does not appear in any other derivation either and is attributed to the choice between SI and CGS.

$$\rho(k)=\frac{1}{V}\sum_j q_j e^{\frac{-k^2}{4\alpha}}$$

$$\phi(k)=\frac{4\pi}{k^2}\frac{1}{V}\sum_j q_j e^{\frac{-k^2}{4\alpha}}$$

$$\phi(r)=\sum_k \phi(k)e^{ikr}$$

$$\phi(r)=\frac{4\pi}{V}\sum_k\sum_j \frac{q_j}{k^2}e^{\frac{-k^2}{4\alpha}}e^{ikr}$$

$$U_{long}=\frac{2\pi}{V}\sum_k\sum_i\sum_j \frac{q_i q_j}{k^2}e^{ik\bullet(r_i-r_j)}e^{\frac{-k^2}{4\alpha}}$$

Ewald Sum:

$$U=U_{short}+U_{long}-U_{self}$$

$$U=\frac{1}{2}\sum_i\sum_j\sum_n \frac{q_i q_j}{\left|r_i-(r_j+nL)\right|}erfc\left(\sqrt{\alpha}\left(r_i-(r_j+nL)\right)\right)+\frac{2\pi}{V}\sum_k\sum_i\sum_j \frac{q_i q_j}{k^2}e^{\frac{-k^2}{4\alpha}}e^{ik\bullet(r_i-r_j)}-\left(\frac{\alpha}{\pi}\right)^{\frac{1}{2}}\sum_i q_i^2$$

NO. OF COPIES ORGANIZATION

1 (PDF ONLY) DEFENSE TECHNICAL INFORMATION CTR
DTIC OCA
8725 JOHN J KINGMAN RD
STE 0944
FORT BELVOIR VA 22060-6218

1 US ARMY RSRCH DEV & ENGRG CMD
SYSTEMS OF SYSTEMS INTEGRATION
AMSRD SS T
6000 6TH ST STE 100
FORT BELVOIR VA 22060-5608

1 DIRECTOR
US ARMY RESEARCH LAB
IMNE ALC IMS
2800 POWDER MILL RD
ADELPHI MD 20783-1197

1 DIRECTOR
US ARMY RESEARCH LAB
AMSRD ARL CI OK TL
2800 POWDER MILL RD
ADELPHI MD 20783-1197

2 DIRECTOR
US ARMY RESEARCH LAB
AMSRD ARL CS OK T
2800 POWDER MILL RD
ADELPHI MD 20783-1197

2 DIRECTOR
US ARMY RESEARCH LAB
AMSRD ARL CI J GOWENS
R NAMBURU
2800 POWDER MILL RD
ADELPHI MD 20783-1197

ABERDEEN PROVING GROUND

1 DIRECTOR
US ARMY RSCH LABORATORY
ATTN AMSRD ARL CI OK (TECH LIB)
BLDG 4600

1 DIRECTOR
US ARMY RSCH LABORATORY
ATTN AMSRD ARL CI H C NIETUBICZ
BLDG 328

NO. OF COPIES ORGANIZATION

6 DIRECTOR
US ARMY RSCH LABORATORY
ATTN AMSRD ARL CI HC J CLARKE
P CHUNG (5 CYS)
BLDG 394